On the Prediction of Ultimate Separation in Parametric Pumps

Quantitative theories based on first principles are derived to explain the roles of heat and mass transfer in the attainment of steady state or ultimate separation in closed direct-thermal-mode parametric pumps. The theoretical results are in agreement with applicable experimental data, including the experimental anomaly called *reversed separation*. Under conditions when the axial dispersion is much greater than molecular diffusion, the theory predicts and experiments confirm that $1/\ln(\alpha_z)$ varies in a linear way with fluid displacement at constant frequency. An additional asymptotic result suggests that when $Sh >> Pe_M$, there is a simple linear connection between $1/\ln(\alpha_\infty)$ and Pe_M which is supported by experimental data.

S. C. FOO and R. G. RICE

Department of Chemical Engineering
University of Queensland
St. Lucia, Brisbane, Australia, 4067

SCOPE

Parametric pumping is by now a well-known separation technique whereby periodic transfer is coupled in a synchronous way to a periodic velocity field. It was developed by Wilhelm and co-workers in 1966. The original and subsequent researchers (Wilhelm et al., 1968; Pigford et al., 1969; Sweed and Wilhelm, 1969; Sweed and Gregory, 1971) have been concerned mainly with predicting the transient response. In recent times (Horn and Lin, 1969; Gregory and Sweed, 1970; Chen and Hill, 1971), researchers have been coming to grips with the question of continuous operation. It is here that the ultimate separation enters the picture, since the transient approach to steady state is of little significance. Questions then arise regarding the existence of an optimum selection of fluid displacement (amplitude) and frequency (Rice, 1973; Rice and Foo, 1974; Rice, 1975). Moreover, the question of phase difference has never been given a firm theoretical footing. In the present study we undertake to answer these questions.

In the direct-thermal-mode of operation, a solid adsorbent with a temperature-dependent affinity for the solute to be separated is used as a retardation media, while periodic fluid motion pumps the lean solvent phase (cold cycle) and rich solute phase (hot cycle) to their respective reservoirs. During the first part of a cycle, the steps involved include first the transient cooling of the packed bed; this causes solute migration from the bulk phase to the solid adsorbent. In this journey, the solute is retarded by a film resistance at the surface of the solid and dispersed by the action of the applied fluid motion. Some solute moves into the solid by pore diffusion, adsorbing on the pore walls along the way.

In the second part of the cycle (hot cycle), the solute desorbs and wends its way back to the bulk phase in exact reverse of the preceding steps. The rate of solute movement depends on the local bed temperature, which determines the equilibrium driving force for mass transfer. This fundamental picture has been recently used (Rice, 1975) to evolve a quantitative theory to predict the magnitude of concentration difference at ultimate separation ($t \rightarrow \infty$) between the lean and rich reservoirs in a parametric pump. Notwithstanding the reasonable comparison with experiment using only parameters calculated from first principles, there are serious questions regarding the generality of this theory, especially the assumption that the axial concentration profile is linear. Furthermore, the aforementioned theory precludes the occurrence of an equilibrium pinch type of thermodynamic limitation, since the form taken by the linearized adsorption isotherm is such that at different temperatures, isotherms are required to be parallel.

The analytical model presented in the present study differs from the former approach in several respects. While building on the apparent successes of the earlier model (Rice, 1975), we derived a more realistic axial concentration profile to show an exponential dependence. Furthermore, equilibrium isotherms were not assumed to be parallel. Finally, as a strong test for the new theory, the curious reversed-separation phenomenon (Rice and Mackenzie, 1973) is theoretically examined and explained in terms of heat and mass transfer phase differences. The consequences of imposing a thermal phase lead are reexamined in the light of the new theory.

CONCLUSIONS AND SIGNIFICANCE

A fundamental frequency analysis of the closed direct-thermal-mode parametric pump has led to a comprehensive theory to predict ultimate separation factor under conditions of purely sinusoidal potentials. It is confirmed experimentally that the theory can be used to estimate events under conditions of square-wave potentials. The dependence of optimum separation factor ($\alpha_{z,\text{opt}}$) over a significant frequency band can be described by the simple relation $AR\omega/\mathcal{D} =$ constant, where the constant depends on system physical dimensions. A significant consequence of the theory, confirmed by a limited number of experiments, shows that $1/\ln(\alpha_z)$ depends in a linear way on fluid displacement at constant frequency. Under conditions such that $Sh >> Pe_M$, it was also demonstrated that $1/\ln(\alpha_z)$ is a linear function of Peclet number at constant fluid amplitude. It is suggested that these two asymptotic results can be used for direct parameter estimation and for scale-up purposes of specific systems. It is concluded that significant liquid separations are not expected when $Pe_M > 100$, irrespective of magnitude of fluid displacement and of thermal phase lead.

Correspondence concerning this paper should be addressed to R. G. Rice.

The main thrust of parapump research in recent years has been directed at explaining the concentration buildup experienced during the transient phase of operation. Work on this area has been recently reviewed (Wankat, 1974). Perhaps the singularly most important contribution along these lines has been the elementary equilibrium theory of Pigford, Baker and Blum (1969), later modified by Aris (1969). This work clearly explains the reasons for separation, and the method of analysis put forth by Pigford et al. has since become very popular. Owing to the many idealizations implicit to the equilibrium model, it cannot be used to predict ultimate separation. In truly continuous operation of parapumps, the transient response is not significant; however, several researchers (Gregory and Sweed, 1970; Chen and Hill, 1971) have used the equilibrium model to delineate conditions under which large separations can be expected. Nonetheless, the a priori prediction of the magnitude of separation cannot be calculated unless the fundamental transport dissipative effects are embedded in the analysis, especially the explicit dependence on frequency and fluid displacement. In the present study we build on the theoretical analysis in previous studies (especially Rice, 1975), striking out those assumptions proving to be contentious and adding insight gained from recent laboratory experimentation (Mackenzie, 1972; Jones, 1974).

THEORY

One of the purposes of any theoretical analysis is the attempt to discover anomalous behavior of a physical system. Badly behaved mathematical models are unexpected, especially if the physical system under analysis is nonreactive and is operated (normally) very slowly. In previous communications (Rice, 1973; Rice and Foo, 1974; Rice, 1975), it was theoretically predicted (and only partially confirmed experimentally) that a closed, direct-thermal-mode parapump suffers a maximum in ultimate separation which depends on the values taken by the independent variables fluid displacement (amplitude) and frequency of operation. Indeed, it was predicted (Rice, 1973) that a reversed separation can occur at high frequency, small amplitude. The theoretical suggestion of high frequency operation (hence faster transient response) has not been widely exploited for liquid systems, save for the few experiments of Mackenzie and Rice (1973) where the interesting reversed separation was indeed found to occur. Unfortunately, at the time the available theory was unable to predict with any degree of certainty the frequency and amplitude required to produce the experimentally observed reversal.

Prediction of unexpected physical phenomena, such as reversed separation, would appear to be a strong test for new theories purporting to explain the quantitative nature of ultimate separation. In the present study, a new theory is developed which accurately predicts reversed separation and, more importantly, compares favorably with available literature data. The new theory shows a distinctly large maximum, followed by a highly attenuated minimum, as frequency increases. On consideration of the frequency response of distributed parameter systems, certainly such resonance as described above is not unexpected. What we hope to learn from the exercise is that a bad selection of frequency and fluid amplitude is distinctly probable.

The approach we take here is to develop steady state models of the ultimate separation, that is, the state of the system whereby the time-average solute composition in the parapump reservoirs remain stationary. Under such conditions, the time-average flux over the active length of column is required to be nil; otherwise, separation would continue. The limit called *ultimate separation* occurs owing to certain dissipative effects inherent in the process.

The main dissipative effects, in their relative order of importance, are pore diffusion, film transfer resistance, axial dispersion, and interparticle mass and heat diffusion. Thermodynamic effects arising from the type of adsorption isotherm obtaining are of equal importance but are usually nonlinear and hence analytically intractable. Nonetheless, there would appear to be an underlying but simple driving force for separation which can be closely approximated by a linear type of isotherm.

The model we now present includes the effects of pore diffusion within the solid adsorbent, film mass transfer resistance at the solid–bulk fluid boundary, and axial dispersion arising from the periodic motion of the bulk fluid. The heat transfer between the jacket surrounding the bed and the bed itself is assumed to obey simple, first-order, lumped parameter dynamics. A more rigorous treatment is also presented whereby the phase margin and attenuation between jacket temperature and average bed temperature are obtained from solution of the dynamic thermal diffusion equation including a heat transfer resistance at the boundary of bed and jacket. This gives rise to a two-parameter phase relation. Owing to sparsity of temperature response information in reported literature data, the lumped parameter thermal model is used for comparison of theory and experiment.

The usual chromatographic equations are used to describe the system. Thus, the mass balance for porous solid spheres filled with fluid in a packed bed is taken as

$$\frac{\partial C^*}{\partial t} + \rho_s \left(\frac{1-\epsilon_p}{\epsilon_p} \right) \frac{\partial q}{\partial t} = \mathcal{D}_p \frac{1}{r_s^2} \frac{\partial}{\partial r_s} r_s^2 \frac{\partial C^*}{\partial r_s} \quad (1)$$

subject to

$$-\mathcal{D}_p \frac{\partial C^*}{\partial r_s}\bigg|_{r_s=R_s} = k_c (C - C^*|_{r_s=R_s})$$

and

$$\frac{\partial C^*}{\partial r_s}\bigg|_{r_s=0} = 0$$

and the mass transfer rate between bulk fluid and solid can be represented by

$$\frac{\partial C}{\partial t} + V(t) \frac{\partial C}{\partial x} + \frac{k_c a}{\epsilon_b} (C - C^*|_{r_s=R_s}) = \mathcal{D}^* \frac{\partial^2 C}{\partial x^2} \quad (2)$$

where C^* denotes the fluid composition in equilibrium with the local solids composition q, and C represents the local bulk or flowing fluid composition. Later, results are also given for a simple lumped parameter description of the rate process described by Equation (1). Equilibrium between solid and fluid is assumed linear:

$$q = k(T) C^* \quad (3)$$

The temperature dependence of $k(T)$ is such that

$$k(T) = k_o + k_1 T \quad (4)$$

where normally k_1 is expected to be negative.

Temperature and velocity are periodic; hence, fluid composition is expected to be periodic. A general functional form for the dependent variables is suggested by the periodic nature of the above transport equations; that is,

$$C^*(x, r_s, t) = \sum_{n=-\infty}^{n=\infty} C_n^*(x, r_s) e^{in\omega t} \quad (5)$$

and similarly for the remaining dependent variables. As a first approximation, we neglect harmonics higher than first and represent the system as comprised of a steady plus a deviation from steady state which is purely sinusoidal; that is,

$$C^*(x,r,t) = \overline{C}^*(x,r_s) + C^*{}_{+1}(x,r_s)e^{i\omega t} + C^*{}_{-1}(x,r_s)e^{-i\omega t} \quad (6)$$

$$C(x,t) = \overline{C}(x) + C_{+1}(x)e^{i\omega t} + C_{-1}(x)e^{-i\omega t} \quad (7)$$

$$V(t) = \frac{A\omega}{2}e^{i\omega t} + \frac{A\omega}{2}e^{-i\omega t} \quad (8)$$

where C_{-1} is the complex conjugate of C_{+1}. The form of the assumed solution forces the dependent variables to be real.

While the majority of experimental parapumps have claimed to use square velocity and applied temperature fields, it would seem that actual bed temperature is more nearly sinusoidal than square owing to attenuation and dispersion arising from thermal diffusion and heat transfer resistances. It is an easy matter to calculate contributions from higher harmonics, but for the estimation purposes intended here we shall use only the primary frequency.

The axial coordinate x is measured from the bottom entrance to the bed; hence, when velocity is positive, the bed is cooled and the deviation of temperature from steady state is negative. We symbolically operate in this way so that the solute is concentrated in the bottom reservoir and depleted from the top. If density driven flow is unimportant, the theory holds if we reverse this mode of operation.

If the temperature gradient along the axis is small, the local bed temperature can be represented by the diffusion equation

$$\frac{\partial T}{\partial t} = \alpha_e \frac{1}{r}\frac{\partial}{\partial r} r \frac{\partial T}{\partial r} \quad (9)$$

with transport resistance at the boundary

$$h_w(T_j - T_{r=R}) = k_e \frac{\partial T}{\partial r_{r=R}} \quad (10)$$

Hence, if the jacket and local bed temperature are expected to be purely sinusoidal

$$T_j = \overline{T} - \frac{\Delta T}{2}e^{i\omega t} - \frac{\partial T}{2}e^{-i\omega t} \quad (11)$$

$$T = \overline{T} + T_{+1}(r)e^{i\omega t} + T_{-1}(r)e^{-i\omega t} \quad (12)$$

it is easy to show that

$$T_{+1}(\xi) = -\frac{\Delta T}{2}\frac{J_o(\lambda_{+1}\xi)}{J_o(\lambda_{+1}) - \lambda_{+1}J_1(\lambda_{+1})/Nu}$$

The average bed temperature fluctuation can be calculated from this, in complex notation:

$$\langle T_{+1}\rangle = \frac{\int_o^1 T_{+1}(\xi)\,\xi\,d\xi}{\int_o^1 \xi\,d\xi} = \frac{-\Delta T\,J_1(\lambda_{+1})/\lambda_{+1}}{J_o(\lambda_{+1}) - \dfrac{\lambda_{+1}J_1(\lambda_{+1})}{Nu}}$$

This would seem to be the correct manner of representing average bed temperature, especially at high frequency where phase differences between jacket and bed temperature can be quite large. However, this distributed type of thermal model poses a difficult parameter estimation problem associated with extracting values of Nu and λ_{+1}. Later, in comparing experimental results, we use a simple lumped model to describe thermal effects, the development of which follows.

Normally, there is insufficient information in the literature to estimate both Nu and λ_{+1}; hence, we must be content to represent the bed response with a simple lumped model; that is

$$\frac{dT}{dt} = \left(\frac{h_w A_w}{M_b C_p}\right)[T_j(t - \tau_D) - T] \quad (13)$$

where $(t - \tau_D)$ reflects a time delay inherent in the thermal response. This model gives thermal oscillation as

$$T(t) = \overline{T} - \tfrac{1}{2}T_b e^{i(\omega t+\gamma)} - \tfrac{1}{2}T_b e^{-i(\omega t+\gamma)} \quad (14)$$

where the magnitude is

$$T_b = \frac{\Delta T}{\sqrt{(\tau_b\omega)^2 + 1}}$$

and the phase difference between jacket and bed is

$$\gamma = \tan^{-1}(-\omega\tau_b) - \tau_D\omega + \gamma_L$$

where γ_L is incorporated to allow for the possibility of an applied phase lead.

Inserting the functional forms given by Equations (6), (7), (8) and (14) into the defining Equations (1) to (4), and neglecting harmonics higher than first, we get for the steady part

$$\frac{A\omega}{2}\frac{d}{dx}(C_{+1} + C_{-1}) = \mathcal{D}^*\frac{d^2\overline{C}}{dx^2} = A\omega\frac{dC_R}{dx} \quad (15)$$

where $C_R(x)$ is the real part of $C_{+1}(x)$, and the steady diffusion equation requires

$$\overline{C}^*(1,x) = \overline{C}(x) \quad (16)$$

Furthermore, the functions describing the excursions from from steady state in the adsorbent particle can be shown to be the solution of

$$\frac{\partial^2 C^*{}_{+1}}{\partial\xi_s} + \frac{2}{\xi_s}\frac{dC^*{}_{+1}}{\partial\xi_s} - i(1 + H_o)\,Pe_p\,C^*{}_{+1} = -i\,H_1\,Pe_p\,\overline{C}(x)\,T_b\,e^{i\gamma} \quad (17)$$

with the boundary conditions for symmetry and finite resistance; that is

$$\left.\frac{\partial C^*{}_{+1}}{\partial\xi_s}\right|_{\xi_s=1} = Nu_p(C_{+1} - C^*{}_{+1})|_{\xi_s=1};$$

$$\left.\frac{\partial C^*{}_{+1}}{\partial\xi_s}\right|_{\xi_s=0} = 0 \quad (18)$$

The convective equation is taken to be (in perturbation variables)

$$\frac{A\omega}{2}\frac{d\overline{C}}{dx} + i\,\omega\,C_{+1} + \left(\frac{k_c a}{\epsilon_b}\right)[C_{+1}(x) - C^*{}_{+1}(1,x)] = 0 \quad (19)$$

where the dispersion term is neglected in the latter expression, being considered significant only as it affects the steady profile $\overline{C}(x)$.

The solutions of the above equations, if we assume the time-average reservoir compositions to be constant [that is, $\overline{C}(0) = C_{\text{BOT}}$, $\overline{C}(L) = C_{\text{TOP}}$] are found to be

$$\overline{C}(x) = C_B - \frac{C_B - C_T}{1 - e^{uL}}(1 - e^{ux}) \quad (20)$$

$$C^*{}_{+1}(\xi_s,x) = \frac{Nu_p\left[C_{+1} - \dfrac{\tfrac{1}{2}H_1\overline{C}(x)\,T_b e^{i\gamma}}{1 + H_o}\right]}{z_{+1}\cot(z_{+1}) - 1 + Nu_p}\left(\frac{\sin(z_{+1}\xi_s)}{\xi_s\sin(z_{+1})}\right)$$

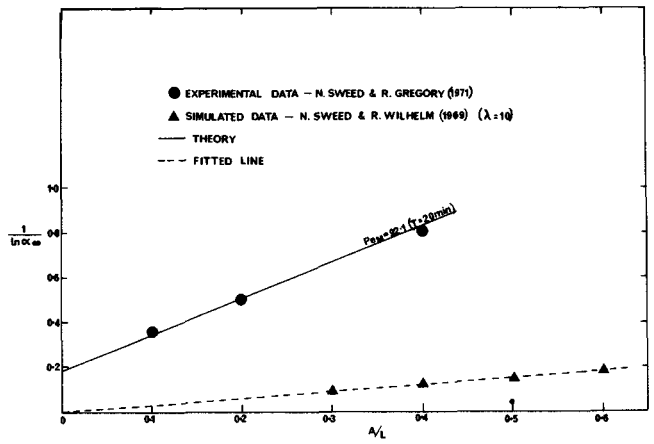

Fig. 1. Comparison of isofrequency experimental results with theory [Equation (27)]. The Sweed-Wilhelm parameter λ is proportional to Sh/Pe_M.

$$+ \frac{\frac{1}{2} H_1 \overline{C}(x)\, T_b e^{i\gamma}}{1 + H_o} \qquad (21)$$

from which the sought after periodic deviation from steady state of the bulk composition $C_{+1}(x)$ is found to be

$$C_{+1}(x) = -\psi_1 \overline{C}(x) - \psi_2 \frac{d\overline{C}}{dx}\left(\frac{A\omega}{2}\frac{R^2}{\mathcal{D}}\right) \qquad (22)$$

A detailed description of the complex functions $\psi_1(z_{+1})$ and $\psi_2(z_{+1})$ is given in Appendix A.

In developing our steady (for example, $\overline{C}$) and perturbation (for example, C_{+1}) functions, we have tacitly taken the following line of reasoning. At the ultimate steady state ($t \to \infty$), the steady nonperiodic part of the solution [that is, $\overline{C}(x)$] is influenced mainly by dissipative effects associated with axial dispersion, since the steady gradient along the axis is expected to be large. On the other hand, the (relatively) fast changing periodic mass transfer around an adsorbent particle is dissipated mainly by film resistance and pore diffusion, with negligible local effects owing to axial dispersion. Thus we have disregarded axial dispersion effects in the equations for C_{+1} and C^*_{+1}, including such effects in the equation for $\overline{C}(x)$. It is difficult to assess the quantitative mathematical implications of these assumptions; however, the engineering intuition and physical reasoning outlined above would appear to be reasonable under the conditions existing at steady state. The aim is to obtain engineering estimates which explain to a reasonable degree a wide range of experimental results. With due consideration to these aims, it would seem that a favorable comparison of theory and experiment is an acceptable justification for these assumptions.

CALCULATION OF ULTIMATE SEPARATION

The ultimate separation is calculated from the well-known experimental fact that the time-average axial flux tends to zero as the ultimate (time-average) composition of the connecting reservoirs is approached. Mathematically, the axial flux can be represented by

$$J = -\mathcal{D}^* \frac{\partial C}{\partial x} + V \cdot C \qquad (23)$$

the time-average of which after the known functions are inserted in Equations (7) and (8) is

$$\langle J \rangle = 0 = -\mathcal{D}^* u \left(\frac{C_B - C_T}{1 - e^{uL}}\right) e^{ux} + \langle V \cdot C \rangle \qquad (24)$$

where u is negative and real:

$$u = -\frac{A\omega \text{ Real } [\psi_1]}{\mathcal{D}^* + \frac{(A\omega)^2}{2}\frac{R^2}{\mathcal{D}} \text{ Real } [\psi_2]} \qquad (25)$$

The time-average convective term is easily seen to be

$$\langle V \cdot C \rangle = \frac{A\omega}{2} C_{+1}(x) + \frac{A\omega}{2} C_{-1}(x) = A\omega\, C_R(x) \qquad (26)$$

By rearranging Equation (24), the separation factor $\alpha_\infty = C_B/C_T$ can be extracted to give

$$\ln(\alpha_\infty) = -uL = \frac{(L/R)^2\, Pe_M\, (A/L) \text{ Real } [\psi_1]}{\frac{\mathcal{D}^*}{\mathcal{D}} + \frac{1}{2}(L/R)^2\, Pe_M{}^2 (A/L)^2 \text{ Real } [\psi_2]} \qquad (27)$$

which is independent of axial position. The proof of this rather tedious manipulation is given in Appendix B. The complex transcendental functions ψ_1 and ψ_2 arise from the intricate coupling of pore diffusion and bulk phase transport. Thermal phase lead can effectively be considered by summing the actual physical phase lag with any value of phase lead; hence, γ can be used as a design parameter.

Equation (27) is thus the sought after connection between frequency (represented by a dimensionless Peclet number $Pe_M = R^2\omega/\mathcal{D}$), amplitude (or dimensionless fluid displacement A/L), and system physical properties.

A simpler approach to the problem would be to lump film and pore resistance (see Perry, 1963) and hence replace the distributed pore diffusion, Equation (1), with the lumped model

$$\alpha_b \frac{\partial q}{\partial t} + (\beta_b - 1)\frac{\partial C^*}{\partial t} = \frac{k_c a}{\epsilon_b}(C - C^*) \qquad (28)$$

Following the same procedure as the exercise leading to Equation (27), yields results for the lumped model that can be shown to give the following relationship for ultimate separation factor:

$$\ln \alpha_\infty = \frac{(L/R)^2\, Pe_M (A/L) \text{ Real } [\phi_1]}{\frac{\mathcal{D}^*}{\mathcal{D}} + \frac{1}{2}\left(\frac{L}{R}\right)^2\left(\frac{A}{L}\right)^2 Pe_M{}^2 \text{ Real } [\phi_2]} \qquad (29)$$

This has a functional form identical to the pore diffusion result, Equation (27). The simpler transcendental functions ϕ_1, ϕ_2 are presented in Appendix A. If we introduce an expression for the ratio of axial dispersion to molecular diffusion (after Klinkenberg and Sjenitzu, 1956)

$$\frac{\mathcal{D}^*}{\mathcal{D}} = 1 + \frac{3}{\sqrt{2}}(D_s/R)(L/R)(A/L)\, Pe_M \qquad (30)$$

into Equations (27) and (29) and if the second term in Equation (30) (arising from the fluid mixing) is large compared to unity, then the inverse of the logarithm of separation factor equations leads to the simple form

$$\frac{1}{\ln \alpha_\infty} = a_o(A/L) + b_o \qquad (31)$$

where a_o, b_o are proper constants when frequency is constant. This would appear to be a very useful result, allowing both a check on the theory and a convenient method

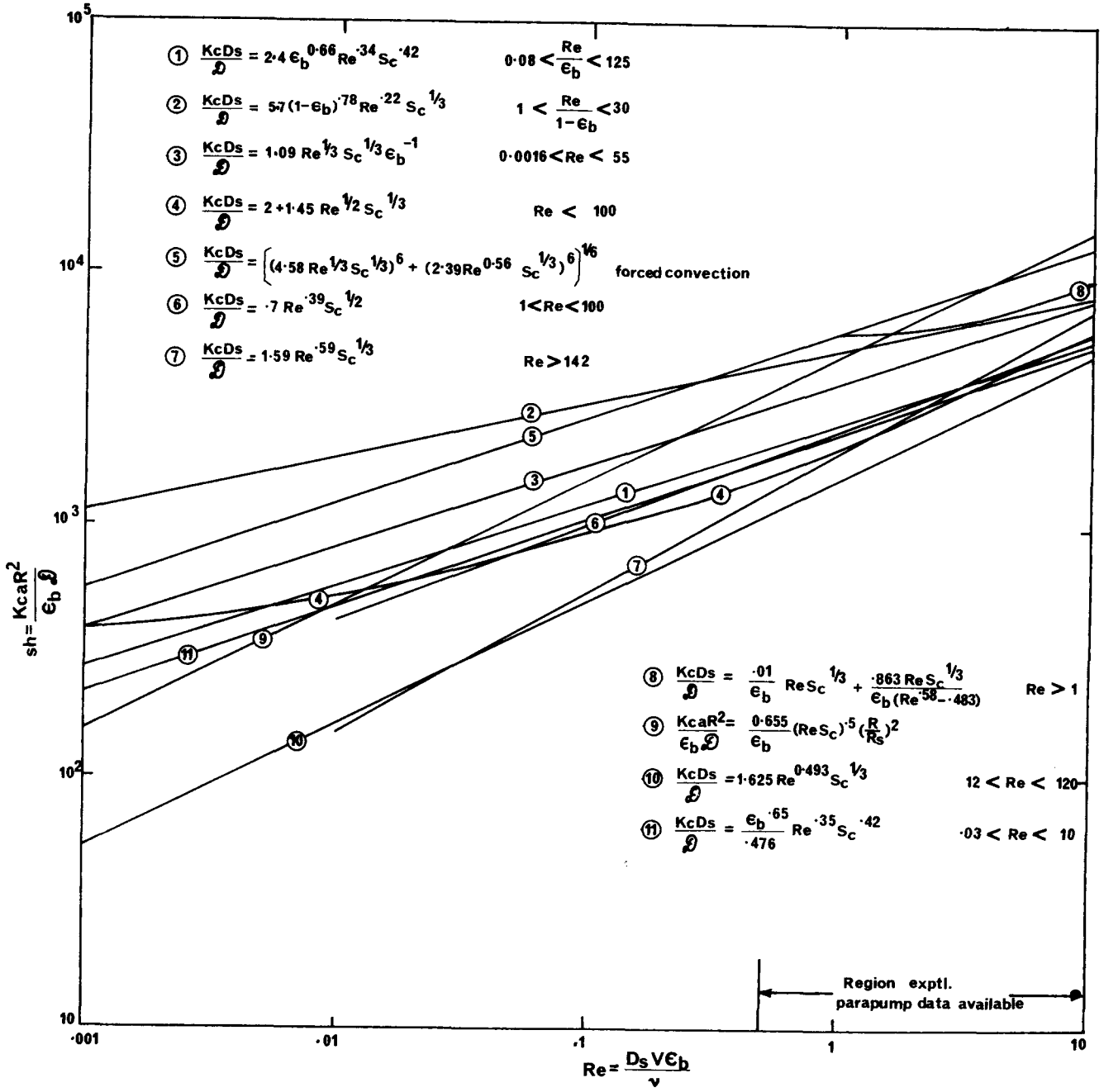

Fig. 2. Packed bed mass transfer correlations for $Sc = 483$, curve number-reference: (1) Williamson et al. (1963), (2) Chu et al. (1953), (3) Wilson and Geankoplis (1966), (4) Wakao et al. (1958), (5) Kaabelas et al. (1971), (6) Kasaoki and Nitta (1969), (7) Jolis and Hanratty (1969), (8) Gupta and Thodos (1962), (9) Perry's Handbook (4 ed.) (10) McCune and Wilhelm (1949), (11) Gaffney and Drew (1950).

for direct parameter estimation. This simple approximate result is tested in Figure 1 with experimental and simulated data from the literature. Under conditions that $Sh >> Pe_M$, it can also be shown that one expects

$$\frac{1}{\ln \alpha_\infty} = a_1 Pe_M + b_1 \tag{32}$$

at constant A/L, provided axial dispersion is dominated by convective mixing.

COMPARISON OF THEORY AND EXPERIMENT

The important shortcomings of much reported experimental parapump data arise because (1) most experiments were not conducted long enough to reach ultimate separation (often curve fitting of modest transient equations shows the predicted ultimate separation based on early-time data), (2) there are several physical parameters whose values are not stated, and (3) there is little or no guidance in the most suitable mass transfer coefficient correlation or dispersion relation (Among a selection of many, see Figure 2, for example) to use with the reported data. There is a definite need for a comprehensive bringing together of various estimated dissipative factors in adsorptive types of systems.

In the current work, we use the dispersion relationship of Klinkenberg and Sjenitzer (1956) to describe mixing along the axis [Equation (30)]. However, there is strong evidence that for oscillating flow in simple tubes there is a second-order dependence on amplitude and Peclet number (Harris and Goren, 1967; Rice and Eagleton, 1970):

$$\frac{\mathcal{D}^*}{\mathcal{D}} = 1 + k_p \left(\frac{A}{L} Pe_M\right)^2 \tag{33}$$

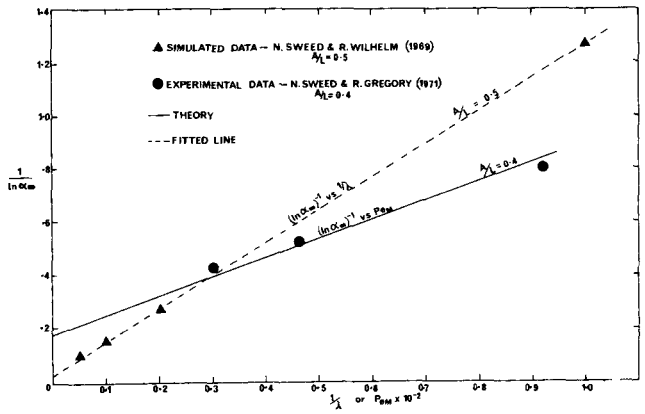

Fig. 3. Comparison of isoamplitude experimental results with theory [Equation (27)]. The Sweed-Wilhelm parameter $1/\lambda$ is proportional to Pe_M/Sh.

Here k_p is a constant which depends on tube (pore) size. One expects this second-order dependence at the low frequencies typical of liquid parapumps. If dispersion is second order in amplitude, then the value of the intercept b_o in the asymptotic relationship [Equation (31)] tends to zero, a behavior exhibited by the simulated data of Sweed and Wilhelm (1969) presented in Figure 1.

In the comparisons we make with certain experiments and the theories embodied in Equations (27) and (29), the mass transfer coefficient will be calculated from the semiempirical correlation of Wakao (1958):

$$\frac{k_c D_s}{\mathcal{D}} = 2 + 1.45\, Re^{1/2}\, Sc^{1/3} \qquad (34)$$

There is a precedent for using this correlation in adsorptive systems (Hashimoto and Smith, 1973), and, more importantly, this correlation has certain other features which are very attractive. In Figure 2 we have recalculated the many correlations suggested for the packed-bed mass transfer coefficient and present them on standardized basis. The Wakao correlation appears to lie in the mean position without exhibiting extreme behavior other than the low Reynolds asymptote. There is strong theoretical justification for the asymptotic ($Re \to 0$) value of 2 for the Sherwood number, and the Wakao work is the only packed-bed correlation of the many considered which includes this important limit.

The solid straight line in Figure 1 was calculated by using the pore diffusion model of ultimate separation, Equation (27). No parameters were fitted, and only first principles (along with the physical properties provided by Sweed and Gregory, 1971, which are listed in Table 1) were used to compute the expected ultimate separation factor α_∞. Admittedly, three data points for comparison purposes cannot be considered conclusive. However, due consideration must be given to the fact that each data point represents several days of experimental work. Nonetheless, the agreement of the isofrequency results appears to be excellent. The additional simulated data of Sweed and Wilhelm plotted in Figure 1 are based on parameters estimated by these workers from actual experimental data at conditions outside the simulated range. These simulated data are thus seen to be very close approximations to real experiments. These simulated data are included in an effort to corroborate the linear dependence predicted by the asymptotic result, Equation (31); the dashed line was not calculated from either Equations (27) or (29) but drawn by eye to illustrate the expected linear dependence.

Table 1. Sweed and Gregory (1971) Physical Data and Estimates

ρ_s	$= 1.1$ g/cm^3
ϵ_b	$= 0.36$
ϵ_p	$= 0.5$
$\frac{H_1 \Delta T}{1 + H_o}$	$= -0.095$
H_o	$= 1.12$
$\frac{\mathcal{D}}{\mathcal{D}_p}$	$= 3.44$
$\frac{L}{R}$	$= 109.1$
$\frac{R}{R_s}$	$= 11$
σ	$= 2.54$
$\frac{\alpha_b k_1 \Delta T}{1 + H_o}$	$= -0.0322$
τ_b	$= 39.1$ s
τ_D	$= 0$ s
Sc	$= 483$
Sh_p	$= 468$

It was mentioned earlier that an asymptotic isoamplitude relationship exists such that $1/\ln \alpha_\infty$ is expected to be linear in Pe_M [Equation (31)]. Inspection of the complex function ψ_1, ψ_2 for the pore diffusion model and ϕ_1, ϕ_2 for the lumped resistance model shows that when Sherwood number >> Peclet number the plot of $1/\ln \alpha_\infty$ vs. Pe_M should produce a linear relationship. The predicted linearity is tested in Figure 3 by again using the experiments of Sweed and Gregory (1971) and the simulated data of Sweed and Wilhelm (1967). As before, the solid line was calculated from first principles by using Equation (27) and physical data listed in Table 1. The dashed line was drawn by eye to illustrate the expected linear dependence.

The comparisons in Figures 1 and 3 clearly point to a simple underlying dependence on frequency (Peclet number) and amplitude (A/L).

In Figure 4 we bring together all of the experimental data of Sweed and Gregory (1971) showing the theoretical predictions over a six decade range of Peclet number. We also include in this figure the optimum operational curve (maximum α_x) for the Sweed-Gregory system. The heavy dashed curve of A/L vs. Pe_M represents the best selection of Pe_M (given a value of A/L) to give maximum α_x, including the fact that A/L is constrained to be $\leqq 0.5$. Values of $A/L > 0.5$ cause the reservoirs to mix from cycle to cycle, an unacceptable method of operation. The heavy solid curve represents the $(\alpha_x)_{opt}$ which corresponds to the best selection of Pe_M. It is clear from this rather comprehensive illustration that the method of operation in the Sweed-Gregory experiments appears to be far from optimum. For example, these workers used an $A/L = 0.4$ and $Pe_M \simeq 30$ giving $\alpha_x = 10$, quite a small separation. Using the same Peclet number and $A/L \simeq 0.011$, the current theory predicts $\alpha_x \simeq 2\,000$, clearly a magnificent improvement. For the Sweed-Gregory system, there is a flat region for $(\alpha_x)_{opt}$ extending from $Pe_M \cong 6.5$ to 40.0. In this region, the connection between optimum A/L and Pe_M is simply

$$(A/L\, Pe_M)_{opt} \cong 0.32 \qquad (35)$$

Outside this region, the connection becomes more complicated, especially at high frequencies. At high frequencies and small amplitude, Figure 4 shows that a reverse separation is expected. This interesting aspect will be considered shortly.

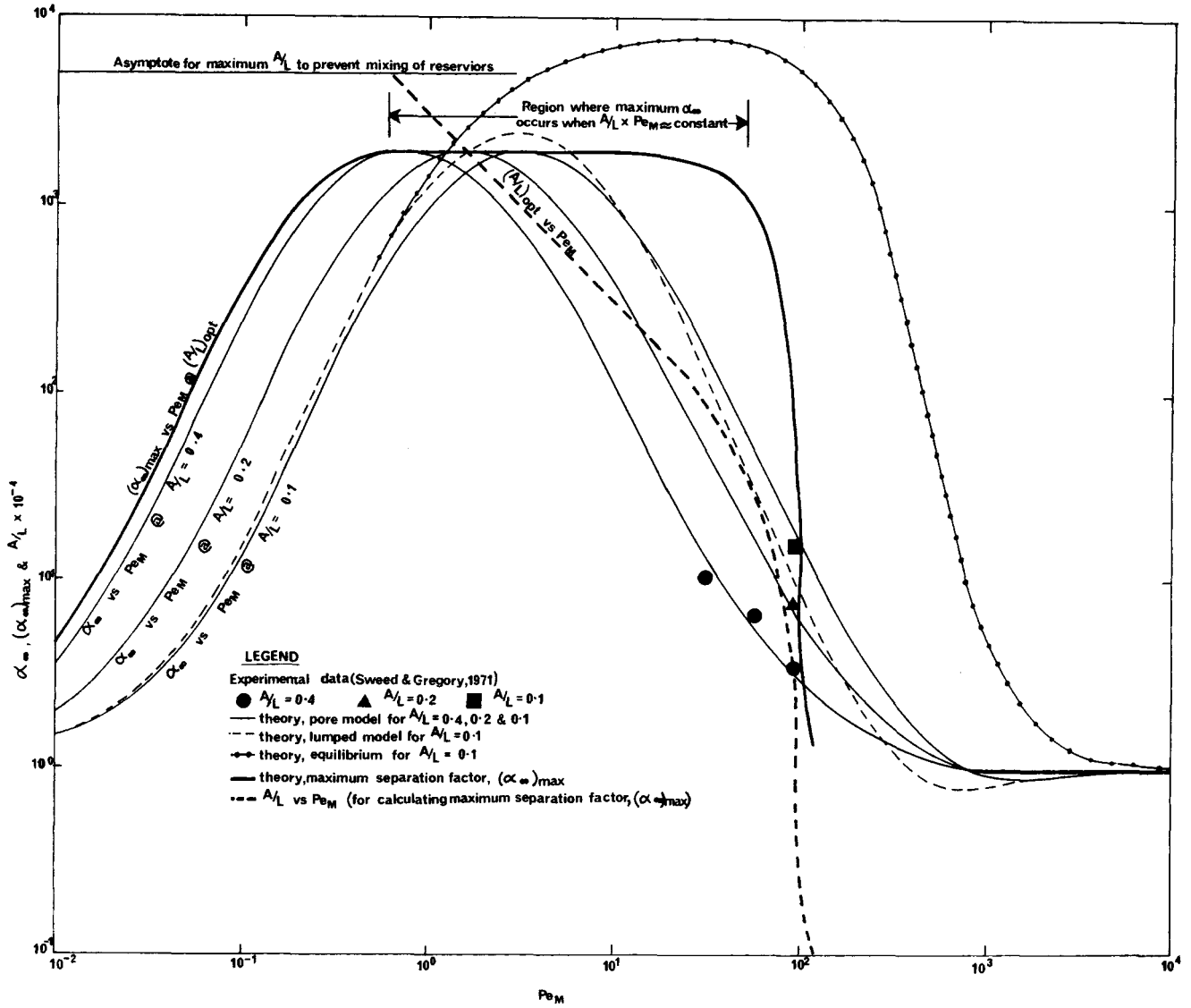

Fig. 4. Predicted performance and maximum separations for the Sweed-Gregory System.

Also shown in Figure 4 are the consequences of using an equilibrium model ($k_c \to \infty$) where it is seen that such an idealization overpredicts α_∞ fivefold at Peclet numbers as small as 7. At higher Pe_M the discrepancy becomes even more severe.

Finally, the effect of lumping pore diffusion into the film coefficient [Equation (29)] on the Sweed-Gregory system is illustrated for $A/L = 0.1$ and compared with the distributed parameter solution [Equation (27)]. The equivalent mass transfer coefficient (to include pore diffusion) used in the lumped model [Equation (29)] was taken to be (Perry, 1963)

$$k_c a = 60 \frac{\mathcal{D}_p \epsilon_p (1 - \epsilon_b)}{D_s^2} \tag{36}$$

where throughout this work we have used a modified packing factor such that only the solid pore area is considered to be effective for mass transfer at the solid fluid interface. Hence

$$a = \frac{6 \epsilon_p (1 - \epsilon_b)}{D_s} \tag{37}$$

The difference in the two models is only significant (for the system considered) at high frequency, where the lumped model predicts the onset of reversed separation (that is $\alpha_\infty < 1$) at a lower frequency (Peclet number) than the distributed model. When we consider the computational tedium associated with more rigorous solution [Equation (27)], it would appear that the simpler lumped model is entirely adequate provided the pore diffusion resistance is reflected in the calculation of effective mass transfer coefficient.

REVERSED SEPARATION

Recently, parapump experiments were performed (Rice and Mackenzie, 1974) on the aqueous oxalic system by using an activated carbon adsorbent. It was the stated intention of this work to explore the possibilities of high frequency operation based on the theoretical prediction (Rice, 1973) that high frequency resonance may give large separations at small amplitudes. Indeed, the cycle time of order 3 minutes produced reversed separations regardless of the manner of operation (cold upflow, hot upflow). What is meant by reversed separation is as follows. If one synchronously forces the bed to be cold during upflow (retarding the solute) and hot during downflow (releasing the solute), one naturally expects the solute to be pumped toward the bottom of the column and ultimately captured and held by the lower reservoir. However, the reverse occurred in the aforementioned experiments; hence, the

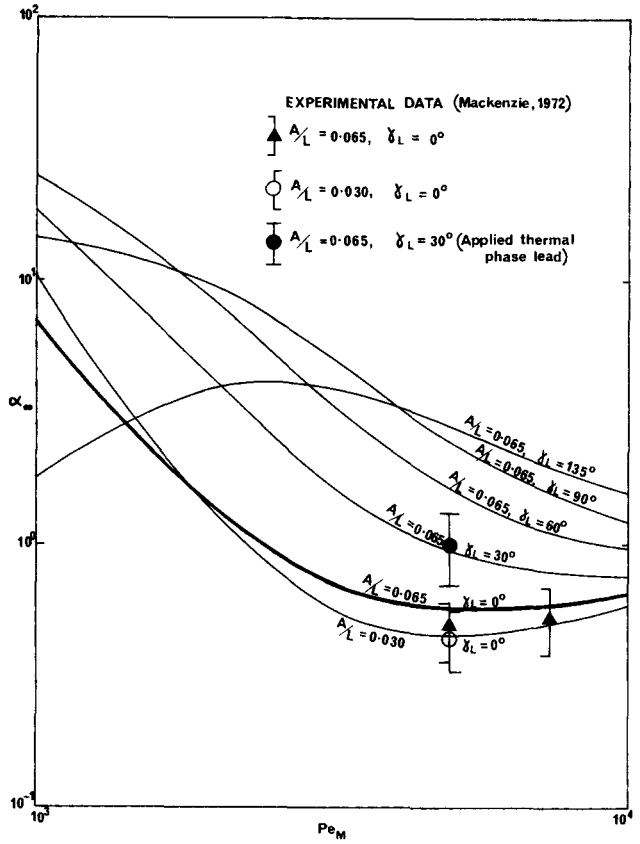

Fig. 5. Prediction of reversed separation for the Mackenzie system.

annotation reversed separation. Theoretical analysis to date has not explained the curious reversed separation, but intuitively one expects that the effect arises from mass and heat transfer phase differences. We now use the Mackenzie (1972) data to test the previously developed theory [Equation (27)]. Table 2 lists physical data, including an estimate of pore diffusion in the porous activated carbon along with the experimental time constant of the bed.

The data for three in-phase experiments and one experiment with an applied 30 deg. thermal phase lead are compared with theoretical predictions in Figure 5. Two in-phase experiments were performed at $A/L = 0.065$, and these are to be compared with the heavy curve representing theoretical predictions. An additional in-phase experiment was performed at $A/L = 0.03$, and, finally, an experiment was performed whereby the jacket temperature was forced to lead velocity by 30 deg. The latter experiment at $A/L = 0.065$ produced no reversed separation.

The comparison of theory with experiment appears favorable indeed, providing a rather strong test for the predictive capacity of the current theory.

It seems obvious now that system thermal lag at high frequency causes the reversed separation, as one expected at the outset. What is rather enlightening about the exercise is the significant effect of applied thermal lead as demonstrated in Figure 5. For example, the effective reservoir composition ratios (large/small) for the $A/L = 0.065$ experiments take values around 1.5. However, the theory shows that if the experiments were performed with an applied thermal lead of 135 deg., a separation factor of between 2 and 3 would have resulted, clearly an improvement. Nonetheless, the theory shows that dissipative forces give rise to a very large attenuation of separation factor at high frequency, and acceptable liquid phase separation factors are not expected when $Pe_M > 100$, regardless of the size of amplitude ratio or the presence of thermal lead.

TABLE 2. MACKENZIE (1972) PHYSICAL DATA AND ESTIMATES

ρ_s	$= 1.7$ g/cm^3
ϵ_b	$= 0.45$
ϵ_p	$= 0.54$
$\frac{H_1 \Delta T}{1 + H_o}$	$= -0.21$
H_o	$= 2.82$
$\frac{\mathcal{D}}{\mathcal{D}_p}$	$= 3.7$
$\frac{L}{R}$	$= 160$
$\frac{R}{R_s}$	$= 5.08$
τ_b	$= 84$ s
τ_D	$= 12$ s
Sc	$= 355$

NOTATION

a = mass transfer area, defined by Equation (37)
A = displacement of interstitial fluid
A_w = heat transfer area between jacket and bed
C = concentration of solute in fluid phase
C_{BOT} = concentration of solute in bottom reservoir
C_{TOP} = concentration of solute in top reservoir
C^* = concentration of solute in equilibrium with adsorbed phase
c_p = heat capacity of bed
D_s = diameter of sorbent particle
$\mathcal{D}$ = molecular diffusion coefficient of solute in fluid phase
$\mathcal{D}^*$ = axial dispersion coefficient of solute in fluid phase
h_w = overall heat transfer coefficient between jacket and bed
$H_o = \dfrac{\rho_s(k_o + k_1 \overline{T})(1 - \epsilon_p)}{\epsilon_p}$
$H_1 = \dfrac{\rho_s k_1 (1 - \epsilon_p)}{\epsilon_p}$
$i = \sqrt{-1}$
J = local axial flux
$J_n(x)$ = bessel function of the first kind of order n
k = slope of linear isotherm, defined in Equation (3)
k_o = adsorption parameter, defined in Equation (4)
k_1 = adsorption parameter, defined in Equation (4)
k_c = mass transfer coefficient, calculated from Equations (34) or (36)
k_e = effective thermal conductivity of bed
L = length of bed
$Nu = \dfrac{h_w R}{k_e}$, Nusselt number for heat transfer
$Nu_p = \dfrac{k_c R_s}{\mathcal{D}_p}$, Nusselt number for pore diffusion
$Pe_H = \dfrac{R^2 \omega}{\mathcal{D}_e}$, Peclet number for heat transfer
$Pe_M = \dfrac{R^2 \omega}{\mathcal{D}}$, Peclet number for mass transfer
$Pe_P = \dfrac{R_s^2 \omega}{\mathcal{D}_p}$, Peclet number for pore diffusion
q = solid composition per unit dry weight of solid
R = column radius
R_s = radius of sorbent particle
r = radial coordinate for column
r_s = radial coordinate for sorbent particle
Sc = Schmidt number

$Sh = \dfrac{k_c a R^2}{\epsilon_b \mathcal{D}}$, Sherwood number for mass transfer

$Sh_p = \dfrac{k_c a R^2}{\epsilon_p \mathcal{D}}$, equivalent Sherwood number for pore diffusion [from Equation (36)]

T = local fluid-solid temperature

T_b = average bed temperature amplitude

T_j = jacket temperature

$\Delta T = (T_H - T_C)/2$, amplitude of jacket temperature

$\overline{T} = (T_H + T_C)/2$, steady temperature

T_C = cold temperature in jacket

T_H = hot temperature in jacket

u = defined by Equation (25)

V = interstitial fluid velocity

x = axial coordinate measured from bottom end of column

$z_{+1} = \sqrt{-i(1 + H_o)Pe_p}$

Greek Letters

$\alpha_b = \rho_s(1 - \epsilon_b)(1 - \epsilon_p)/\epsilon_b$

$\alpha_e = k_e/(\rho C_p)e$, effective thermal diffusivity of bed

$\alpha_\infty = C_{BOT}/C_{TOP}$, ultimate separation factor

$\beta_b = 1 + \epsilon_p(1 - \epsilon_b)/\epsilon_b$

γ = phase angle between thermal and velocity field

γ_L = applied thermal phase lead

ϵ_b = interstitial voidage of bed

ϵ_p = voidage of solid

τ_b = time constant of bed [Equation (15)]

τ_D = time delay of bed [(Equation (15)]

$\delta = \alpha_b(k_o + k_1\overline{T}) + \beta_b$

$\xi = r/R$

$\xi_s = r_s/R_s$

ϕ_1 = as defined in Equation (A-3)

ϕ_2 = as defined in Equation (A-4)

ψ_1 = as defined in Equation (A-1)

ψ_2 = as defined in Equation (A-2)

$\lambda_{+1} = \sqrt{-i\,Pe_H}$

ρ_s = compressed density of solid

ω = frequency

APPENDIX A

The following complex transcendental functions arise in the analysis. For the pore diffusion we define

$$\psi_1 = -\frac{1}{2}\left(\frac{H_1}{1 + H_o}\right) \frac{Sh\ T_b\ e^{i\gamma}\ [z_{+1}\cot(z_{+1}) - 1]}{[z_{+1}\cot(z_{+1}) - 1]\ (Sh + i\ Pe_M) + i\ Nu_p\ Pe_M} \quad \text{(A1)}$$

$$\psi_2 = \frac{z_{+1}\cot(z_{+1}) - 1 + Nu_p}{[z_{+1}\cot(z_{+1}) - 1]\ (Sh + i\ Pe_M) + i\ Nu_p\ Pe_M} \quad \text{(A2)}$$

and for the film controlling model there results

$$\phi_1 = -\frac{1}{2}\left(\frac{\alpha_b k_1}{\delta}\right) \frac{Sh\ T_b\ e^{i\gamma}\ i}{i \cdot Sh - \left(1 - \dfrac{1}{\delta}\right) Pe_M} \quad \text{(A3)}$$

$$\phi_2 = \frac{Sh + i(\delta - 1)\ Pe_M}{i \cdot Sh\ Pe_M\delta - (\delta - 1)\ Pe_M^2} \quad \text{(A4)}$$

APPENDIX B

Having solved the perturbation function $C_{+1}(x)$ and the steady profile $\overline{C}(x)$, the axial mass flux can be calculated by using Equation (23) to give

$$\langle J\rangle = -\mathcal{D}^*\ u\left(\frac{C_{BOT} - C_{TOP}}{1 - e^{uL}}\right) e^{ux} + A\omega\left(C_{BOT} - \frac{C_{BOT} - C_{TOP}}{1 - e^{uL}}\right) \text{Real}\,[\psi_1] - A\omega\left\{\text{Real}\,[\psi_1] + \frac{A\omega}{2}\frac{R^2}{\mathcal{D}}\text{Real}\,[\psi_1]\ u\right\} \left(\frac{C_{BOT} - C_{TOP}}{1 - e^{uL}}\right) e^{ux} \quad \text{(B1)}$$

and by noting that

$$\mathcal{D}^*\ u = -A\omega\ \text{Real}\,[\psi_1] + \frac{A\omega}{2}\frac{R^2}{\mathcal{D}}\text{Real}\,[\psi_2]\ u \quad \text{(B2)}$$

[by inserting the real part of C_{+1} and $\overline{C}$ into (15)]

The time-average mass flux should be nil at ultimate separation; hence Equations (A1) and (A2) show

$$\langle J\rangle = A\omega\left(C_{BOT} - \frac{C_{BOT} - C_{TOP}}{1 - e^{uL}}\right)\text{Real}\,[\psi_1] = 0 \quad \text{(B3)}$$

Since $A\omega = 0$ or Real $[\psi_1] = 0$ would give a trivial solution, the only meaningful solution results when

$$C_{BOT} - \frac{C_{BOT} - C_{TOP}}{1 - e^{uL}} = 0 \quad \text{(B4)}$$

By using the definition of u [Equation (25)], this can be rearranged to give

$$\ln \alpha_\infty = \frac{\left(\dfrac{L}{R}\right)^2\left(\dfrac{A}{L}\right) Pe_M\ \text{Real}\,[\psi_1]}{\dfrac{\mathcal{D}^*}{\mathcal{D}} + \dfrac{1}{2}\left(\dfrac{L}{R}\right)^2\left(\dfrac{A}{L}\right)^2 Pe_M^2\ \text{Real}\,[\psi_2]} = -uL \quad \text{(B5)}$$

LITERATURE CITED

Aris, Rutherford, "Equilibrium Theory of the Parametric Pump", *Ind. Eng. Chem. Fundamentals*, **8**, 603 (1969).

Chen, H. T., and F. B. Hill, "Characteristics of Batch, Semi-continuous and Continuous Equilibrium Parametric Pumps," *Separation Sci.*, **6**, 411 (1971).

Chu, J. C., J. Kalil, and W. A. Wetteroth, "Mass Transfer in a Fluidized Bed," *Chem. Eng. Progr.*, **49**, 141 (1953).

Gaffney, B. J., and T. B. Drew, "Mass Transfer from Packing to Organic Solvents in Single Phase Flow Through a Column," *Ind. Eng. Chem.*, **42**, 1120 (1950).

Gregory, R. A., and N. H. Sweed, "Parametric Pumping: Behaviour of Open Systems Part 1: Analytical Solutions," *Chem. Eng. J.*, **1**, 207 (1970).

Gupta, A., and N. H. Sweed, "Modelling of Nonequilibrium Effects in Parametric Pumping," *Ind. Eng. Chem. Fundamentals*, **12**, No. 3, 335 (1973).

Gupta, A., and George Thodos, "Mass and Heat Transfer in the Flow of Fluids Through Fixed and Fluidized Beds of Spherical Particles," *AIChE J.*, **8**, 608 (1962).

Harris, H. G., and S. L. Goren, "Axial Diffusion in a Cylinder with Pulsed Flow", *Chem. Eng. Sci.*, **22**, 1571 (1967).

Hashimoto, N., and J. M. Smith, "Macropore Diffusion in Molecular Sieve Pellets by Chromatography," *Ind. Eng. Chem. Fundamentals*, **12**, 353 (1973).

Horn, F. J. M., and C. H. Lin, "Parametric Pumping in Linear Column under Conditions of Equilibrium and Nondispersive Flow," *Ber Bunsenges, Phys. Chem.*, **73**, 575 (1969).

Jolis, K. R., and T. J. Hanratty, "Use of Electrochemical Techniques to Study Mass Transfer Rates and Local Skin Friction to a Sphere in a Dumped Bed," *AIChE J.*, **15**, 199 (1969).

Jones, R., B.E. thesis, "Investigations into the Parametric Pumping of Binary Mixtures of Organic Compounds," Univ. Queensland, Australia (1974).

Karabelas, A. J., T. H. Wegner, and T. J. Hanratty, "Use of Asymptotic Relations to Correslate Mass Transfer Data in Packed Beds," *Chem. Eng. Sci.*, **26**, 1581 (1971).
Kasaoki, S., and K. Nitta, "Unsteady State Diffusion within Porous Solid Particles," *Kagaku Kogaku*, **33**, 123 (1969).
Klinkenberg, A., and F. Sjenitzer, "Holding-Time Distribution of the Gaussian Type," *Chem. Eng. Sci.*, **5**, 258 (1956).
Kramers, H., and G. Alberda, "Frequency Response Analysis of Continuous Flow Systems," *ibid.*, **2**, 173 (1953).
Mackenzie, M., B.E. thesis, "The Design and Operation of a Direct Thermal Mode Parametric Pump," Univ. Queensland, Australia (1972).
McCune, L. K., and R. H. Wilhelm, "Mass and Momentum Transfer in Solid-Liquid System, Fixed and Fluidized Beds," *Ind. Eng. Chem.*, **41**, 1124 (1949).
Perry, J. H., ed., *Chemical Engineering Handbook*, 4 ed., pp. 16-12 to 16-13, McGraw Hill, N. Y. (1963).
Pigford, R. L., B. Baker, and D. E. Blum, "An Equilibrium Theory of the Parametric Pump," *Ind. Eng. Chem. Fundamentals*, **8**, No. 1, 144 (1969).
Rak, J. L., J. D. Stokes, and F. B. Hill, "Separations via Semicontinuous Parametric Pumping," *AIChE J.*, **18**, 356 (1972).
Rice, R. G., "Dispersion and Ultimate Separation in the Parametric Pump," **12**, No. 4, 406 (1973).
———., "Transport Resistances Influencing the Estimation of Optimum Frequencies in Parametric Pumps," *Ind. Eng. Chem. Fundamental*, **14**, 202 (1975).
———., and L. C. Eagleton, "Mass Transfer Produced by Laminar Flow Oscillations," *Can. J. Chem. Eng.*, **48**, 46 (1970).
Rice, R. G., and S. C. Foo, "Thermal Diffusion Effects and Optimum Frequencies in Parametric Pumps," *Ind. Eng. Chem. Fundamental*, **13**, No. 4, 396 (1974).
Rice, R. G., and M. Mackenzie, "A Curious Anomaly in Parametric Pumping," *ibid.*, **12**, No. 4, 486 (1973).
Rolke, R. W., and R. H. Wilhelm, "Recuperative Parametric Pumping: Model Development and Experimental Evaluation," *ibid.*, **8**, No. 2, 235 (1969).
Sweed, N. H., and R. A. Gregory, "Parametric Pumping: Modelling Direct Thermal Separations of Sodium Chloride-Water in Open and Closed Systems," *AIChE J.*, **17**, No. 1, 171 (1971).
Sweed, N. H., and R. H. Wilhelm, "Parametric Pumping: Separations via Direct Thermal Mode," *Ind. Eng. Chem. Fundamental*, **8**, No. 2, 221 (1969).
Wakao, N., T. Oshima, and S. Yagi, "Mass Transfer from Packed Beds of Particles to a Fluid," *Chem. Eng. Jap.*, **22**, 780 (1958).
Wankat, P. C., "Cyclic Separation Processes," *Separation Sci.*, **9**, 85 (1974).
Wilhelm, R. H., "Progress Towards the á priori Design of Chemical Reactors," *Pure Appl. Chem.*, **5**, 403 (1962).
———., A. W. Rice, and A. R. Bendelius, "Parametric Pumping: A Dynamic Principle for Separating Fluid Mixtures," *Ind. Eng. Chem. Fundamentals*, **5**, No. 1, 141 (1966).
Wilhelm, R. H., A. W. Rice, D. W. Rolke, and N. H. Sweed, "Parametric Pumping: A Dynamic Principle for Separating Fluid Mixtures," *ibid.*, **7**, No. 3, 337 (1968).
Williamson, J. E., K. E. Bazaire, and C. J. Geankoplis, "Liquid-Phase Mass Transfer at Low Reynolds Numbers," *ibid.*, **2**, 126 (1963).
Wilson, E., and C. Geankoplis, "Liquid Mass Transfer at Very Low Reynolds Numbers in Packed Beds," *ibid.*, **5**, 9 (1966).

Manuscript received March 4, 1975; revision received July 7, and accepted July 8, 1975.

A Coordinate-Transformation Method for the Numerical Solution of Nonlinear Minimum-Time Control Problems

A new method is presented for the numerical solution of nonlinear minimum-time control problems where at least one of the state variables is monotone. A coordinate transformation converts the problem with fixed end point and free end time to one of free end point and fixed end time. The transformed problem can be solved efficiently by the use of the gradient method with penalty functions to force the system to achieve target values of state variables. Application of the method is illustrated by the synthesis of a minimum-time temperature path for the thermally initiated bulk polymerization of styrene.

YOUNG D. KWON*
and
LAWRENCE B. EVANS
Department of Chemical Engineering
Massachusetts Institute of Technology
Cambridge, Massachusetts 02139

Young D. Kwon is with the Chemical Research Center, Allied Chemical Corporation, Morristown, New Jersey 07960.